Spectral Absolute Reflectance of CO_2 Frosts from 0.5 to 12.0μ

B. E. Wood,* A. M. Smith,† J. A. Roux,‡ and B. A. Seiber§
ARO, Inc., Arnold Air Force Station, Tenn.

In situ absolute reflectance measurements have been made for CO_2 frosts formed on LN_2-cooled substrates. Data were obtained spectrally in the wavelength range from 0.5 to 12.0 μ using an infrared integrating sphere. CO_2 frosts were found to exhibit an anomalous dispersion reflectance peak at 4.3 μ which was shown to be a very sensitive indication of the presence of solid CO_2. Also, CO_2 frosts scatter short wavelength ($\lambda < 1.0\ \mu$) radiation significantly and are semitransparent for much of the wavelength range between 2.0 and 12.0 μ. The application of these results to problems associated with cryogenically cooled surfaces is discussed.

Introduction

THE thermal radiative properties of frosts (cryodeposits) on cryogenically cooled surfaces are being studied with increased interest as more and more applications of cryogenic coolants appear. Examples of situations where knowledge of these properties is important are: 1) simulation of cold outer space in ground test facilities by LN_2-cooled black surroundings, 2) reflective and emissive properties of cooled optics, 3) formation of frosts on cold surfaces to approximate the formation of planetary frosts (i.e., polar caps on Mars), 4) variation in transmission of cryogenically cooled optical windows caused by thin film interference effects of thin deposited films, 5) problems associated with absolute calibration of low-temperature black bodies as reference sources, and 6) reduction in visibility through spacecraft windows caused by condensation of water and other contaminants. Previous determinations of these frost properties have suffered somewhat due to the deposits being formed at atmospheric pressure or because the measurements were either obtained by a calorimetric technique or within a narrow wavelength range. This study presents the reflective properties of CO_2 cryodeposits formed on LN_2-cooled surfaces in vacuum. These absolute reflectances were determined in situ and covered the wavelength range from 0.5 to 12.0 μ.

Absolute reflectance measurements of diffusing surfaces in vacuum are ordinarily made using an integrating sphere. These spheres usually have MgO or $BaSO_4$ coatings and their use is limited to wavelengths less than about 2.6 μ because of the low reflectance of the coating for longer wavelengths. However, it was established in Refs. 1 and 2 that the usable wavelength range can be extended if powdered sodium chloride (NaCl) is substituted as the sphere coating. By using the NaCl coating, and developing a new radiation source, the usable wavelength range of the integrating sphere was extended out to 12.0 μ. This instrument was then employed to make cryodeposit reflectance measurements as a function of wavelength λ, deposit thickness τ, deposition rate $\dot{\tau}$, substrate material, and view angle θ relative to the test surface normal.

Received November 18, 1970; revision received March 11, 1971. Presented as Paper 11 at the ASTM/IES/AIAA 5th Space Simulation Conference, Gaithersburg, Md., September 14–16, 1970. This research was sponsored by the Arnold Engineering Development Center, Air Force Systems Command, under Contract F40600-71-C-0002 with ARO, Inc.

* Project Engineer, Aerospace Division, von Kármán Gas Dynamics Facility. Associate Fellow AIAA.

† Research Section Supervisor, Aerospace Division, von Kármán Gas Dynamics Facility. Also Associate Professor of Aerospace Engineering (Part-time), University of Tennessee Space Institute, Tullahoma, Tenn. Member AIAA.

‡ Research Assistant, von Kármán Gas Dynamics Facility and University of Tennessee Space Institute, Tullahoma, Tenn.; presently Senior Engineer, Northrop Corporation, Huntsville, Ala. Member AIAA.

§ Research Physicist, Aerospace Division, von Kármán Gas Dynamics Facility; presently Research Assistant, Colorado State University, Fort Collins, Colo.

Apparatus

The infrared integrating sphere (Fig. 1) was composed of two stainless steel hemispheres 8 in. in diam. Its interior surface was coated with powdered reagent grade NaCl. This coating was applied by first spreading a thin layer of low-vapor-pressure vacuum grease (10^{-11} torr at 300°K) on the inside of the sphere. Then with the grease serving as a bonding agent, the previously ground NaCl was pressed onto the sphere wall until a thickness of approximately 5 mm had been obtained. This technique of coating has the advantage of eliminating highly absorbing water that was present when the water slurry method described in Ref. 1 was used.

In the center of the sphere was the cryosurface which was a hollow, $1 \times 1\frac{1}{2} \times \frac{1}{2}$-in. rectangular, stainless steel block that was cooled by continuously flowing LN_2 through it. The test surface was one of the $1 \times 1\frac{1}{2}$-in. faces and was either polished stainless steel or the same face coated with a black epoxy paint. A copper-constantan thermocouple was silver soldered to the surface to allow monitoring of the test surface temperature. To restrict the cryopumping area to that of only the cryosurface, the LN_2 supply lines inside the chamber were vacuum jacketed. In addition, the entire test surface assembly and LN_2 lines could be rotated without disturbing the vacuum. This allowed reflectance measurements to be made as a function of view angle from 0 to 60°. The pumping system for the sphere consisted of an ion pump and an LN_2-trapped 4-in. oil diffusion pump backed by a mechanical pump. This system allowed chamber pressures in the 10^{-7} torr range to be routinely achieved. Formation of the CO_2 cryodeposit was accomplished by flowing CO_2 gas into the chamber at a known flow rate and allowing the gas to be cryopumped by the cryosurface. The flow system consisted of two calibrated standard leaks with a forepressure of one atmosphere. The deposition rate, $\dot{\tau}$, of the gas depended on the standard leak used.

One of the problems associated with using an infrared integrating sphere is that of obtaining an infrared source which emits enough energy at the longer wavelengths. In this study, a 1000 w tungsten-halogen lamp was enclosed in a housing that was water cooled at both ends. This allowed the middle of the housing to heat up to glowing red thereby providing an extra source of infrared energy and in turn causing the temperature of the lamp's quartz envelope to increase. Since quartz is a good emitter beyond 4 μ, the high-temperature lamp envelope along with the glowing housing provided a substantial infrared radiance. With this arrangement the

source was usable over the wavelength range from 0.3 to at least 25 μ. Radiation from the source was chopped at 13 Hz and focused onto the wall of the integrating sphere after passing through a NaCl window (Fig. 1). After striking the sphere wall behind the test surface face, the radiation was reflected diffusely throughout the sphere so that the portions of the sphere that were not illuminated directly were uniformly irradiated. Radiation reflected from either the test surface or a portion of the wall not directly irradiated was collected by an off-axis paraboloidal mirror and focused on the entrance slit of the monochromator.

The monochromator was a prism type single pass system. For most of the measurements a NaCl prism was employed since it was usable over the entire wavelength range from 0.5 to 12.0 μ. In one set of experiments a CaF_2 prism was used since it has a much higher dispersion than NaCl in the 1–6 μ range. The monochromator and paraboloidal mirror were mounted on a table which could be rotated about the vertical center line of the viewport, thus allowing radiation from either the test surface or sphere wall to be collected. The detector was a Reeder thermocouple which had a sensitivity of 25 μv/μw. From the detector the output was amplified, synchronously rectified, and displayed on a strip chart recorder.

Procedure

The hemispherical-angular technique was used for obtaining absolute reflectance measurements. In this technique the spectral hemispherical-directional reflectance ρ_{hd} is determined from the relation[1]

$$\rho_{hd}(\theta,\lambda) = I_r(\theta,\lambda)/I_i(\lambda) \quad (1)$$

where $I_i(\lambda)$ is the intensity diffusely incident on the test surface and $I_r(\theta,\lambda)$ is the intensity reflected within the small collection solid angle $\Delta\omega$ (0.02 sr) inclined at the angle θ with respect to the test surface normal. The measurements were accomplished by first viewing the center of the sample and obtaining a detector output for a given wavelength. This was followed by viewing a portion of the sphere wall (not directly irradiated) through the same solid angle at the same wavelength and again recording the detector output. Since the sphere wall is uniformly irradiated by multiple reflections, the intensity of the radiation reflected from the sphere wall is equal to the intensity incident on the test surface. The two detector outputs are directly related to $I_r(\theta,\lambda)$ and $I_i(\lambda)$ by the same multiplicative constants which depend on the transfer optics and detection system. Hence, the ratio of the two detector outputs yields $I_r(\theta,\lambda)/I_i(\lambda)$ which, by Eq. (1), is the absolute hemispherical-directional reflectance.

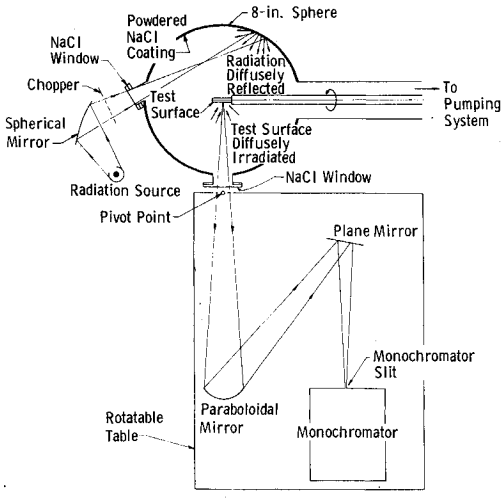

Fig. 1 Schematic of infrared integrating sphere system.

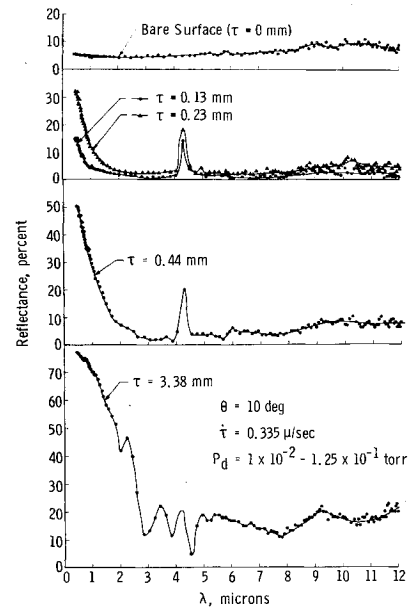

Fig. 2 Reflectance of CO_2 cryodeposits formed on a black epoxy paint substrate.

Prior to the cryodeposit reflectance measurements, the integrating sphere was evacuated to approximately 5×10^{-7} torr. Then, after measuring the reflectance of the bare test surface as a function of wavelength and incidence angle, LN_2 was used to cool the test surface to 94°K. Next, the integrating sphere was valved off from the pumping system and the CO_2 gas flow into the chamber was started. Since the gas could only condense on the test surface, a given flow time resulted in a certain deposit thickness τ. The average thickness over the entire surface could be calculated by knowing the mass flow rate, cryosurface pumping area, and density of deposit. A mass flow rate of either 2.25×10^{-3} g/sec or 2.39×10^{-4} g/sec was used and the cryosurface pumping area was 40.2 cm^2. The cryodeposit density was taken to be 1.67 (Ref. 3) since the deposits were formed at pressures approximately the same as those in Ref. 3. In situ thickness measurements were made in order to verify the deposit thickness as calculated. This was done using the thin film interference techniques discussed in Refs. 3–5. The thicknesses determined by the two methods were in good agreement. Chamber pressures during deposition varied between 10^{-3} and 10^{-1} torr and depended on the flow rate and cryodeposit thickness. For the majority of the deposits the deposition pressure P_d varied between 10^{-2} and 10^{-1} torr. After each thickness of deposit had been formed, reflectance measurements were made over the complete wavelength range from 0.5 to 12.0 μ. This procedure was continued until the deposit had reached a thickness of 3–4 mm.

Results

Black Epoxy Paint Substrate

The reflectances of CO_2 cryodeposits formed on a black epoxy paint substrate are shown in Fig. 2 for wavelengths between 0.5 and 12.0 μ and a view angle of 10°. These deposits were formed using a deposition rate of 0.335 μ/sec which resulted in a deposition pressure of 1×10^{-2} to 5×10^{-2} torr for deposits 0.44 mm thick or less. The structure of the deposits appeared to be polycrystalline. For the 3.38 mm thick deposit the final pressure during deposition was 1.25×10^{-1} torr. The curve in Fig. 2 labeled $\tau = 0$ mm shows the reflectance for the bare black paint substrate viewed in the center at an angle θ of 10° with respect to the surface normal. It is seen that this reflectance is essentially independent of wavelength with there being only a slight increase from 5% up

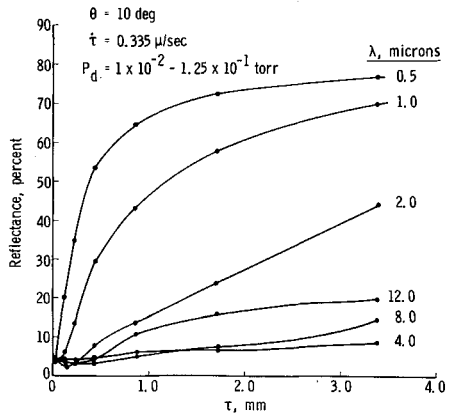

Fig. 3 Reflectance as a function of CO_2 deposit thickness formed on a black epoxy paint substrate.

to 8–9% in the vicinity of 9–11 μ. These results are in good agreement with previous reflectance measurements on black epoxy paint. The other curves in Fig. 2 show the reflectance of cryodeposits ranging from 0.13 mm up to 3.38 mm thick.¶ As can be seen by comparison of the data for different thickness, the reflectance begins to increase first at the short wavelengths ($\lambda < 1.5$ μ) and continues to increase for the long wavelengths as the deposit thickness is increased. The increased reflectance at the shorter wavelengths has been previously reported.[5] For wavelengths greater than about 2.0 μ the reflectance is seen to be less than the bare substrate reflectance for the 0.13 and 0.23 mm thick deposits. This behavior is also typical of the reflectance for shorter wavelengths ($\lambda < 2.0$ μ) but the effect only appears for deposits thinner than those given in Fig. 2. As the deposit thickness is increased further, the reflectance increases for all wavelengths which can be seen in Fig. 2. For the thickest deposit investigated, $\tau = 3.38$ mm, the reflectance has risen to about 77% for $\lambda = 0.5$ μ but drops off rapidly with increasing wavelength.

The single most prominent spectral feature in the curves of Fig. 2 for $\tau = 0.13$, 0.23, and 0.44 mm is the reflectance peak in the wavelength region of 4.3 μ. As the thickness of the deposit increases to 3.38 mm this feature becomes less prominent due to the increase in bulk scattering at other wavelengths around the 4.3μ region. This reflectance peak is attributed to anomalous dispersion[7] wherein a strong absorption band in a liquid or solid has associated with it a very high index of refraction so that both absorption and reflection coefficients are quite high. It is well known that in the gaseous phase, CO_2 exhibits its strongest absorption at 4.25 μ. As can be seen in Fig. 2, the rapid increase in reflectance in this region results in a sensitive technique for identifying the presence of solid CO_2. The peak at 4.3 μ has been seen for deposits as thin as 1 μ.

For deposits less than 3.38 mm thick there is relatively little spectral structure seen in the reflectance spectra in Fig. 2 due to the transmission of the deposit and the highly absorbing black substrate. However, for the 3.38 mm thick deposit the internal scattering has increased significantly which enhances the absorption bands due to the increased reflectance at the nearby wavelengths. Absorption bands can now be seen to occur at 2.0 μ, 2.85 μ and what appear to be bands at 3.85 and 4.55 μ. However, the latter two are really part of the strong absorption band centered around 4.25 μ with the reflectance peak occurring in the middle of the absorption band. Other spectral features to be seen in Fig. 2 for $\tau = 3.38$ mm are a broad reflectance increase extending from 7.9 to 10.5 μ and a gradual rise in reflectance from 10.5 to 12.0 μ. For all of the CO_2 deposits formed on the black substrate, it can be seen that the reflectance will be less than 20% for wavelengths between 2.7 and 12.0 μ. This could be a result of the deposits being highly absorbing or the deposits being somewhat transparent with most of the energy being absorbed by the black substrate. As will be shown later, the latter is the most significant factor.

The reflectance as a function of deposit thickness is presented in Fig. 3 for a view angle of 10° and selected wavelengths of 0.5, 1.0, 2.0, 4.0, 8.0, and 12.0 μ. For 0.5 μ radiation, the 3.38 mm-thick deposit effectively behaves as one of infinite thickness since the reflectance has leveled off. However, for $\lambda = 1.0$ and 2.0 μ, the reflectance is still increasing with thickness at 3.38 mm. The $\lambda = 2$ μ curve is essentially linear with thickness above $\tau = 0.4$ mm. At the other 3 wavelengths, the deposit reflectance is still dependent on thickness at 3.38 mm but much less so than for the 2.0 μ curve. The increase in reflectance for $\lambda = 8.0$ and 12.0 μ is only slight due to the relatively small scattering coefficient at these wavelengths. For the $\lambda = 4.0$ μ curve, very little thickness dependence is present, as expected, since the CO_2 deposit is highly absorbing at this wavelength.

The reflectance dependence on view angle for the deposits discussed in Figs. 2 and 3 is shown in Fig. 4 for wavelengths of 0.5 and 2.0 μ. For the bare black substrate the reflectance at 60° is about 6–7% greater than for a view angle of 0° (e.g., for 0.5 μ radiation the reflectance for 0° is approximately 5% and for 60° is about 11%). For the thicker deposits the reflectance was found to increase by 10–13% as the view angle increased from zero to 60°. It can be seen that the angular dependence is present for all deposit thicknesses and for both wavelengths.

To determine the reflective properties of thin CO_2 deposits on the black epoxy paint and to investigate possible deposition rate effects, a series of measurements was made on deposits formed at a deposition rate, $\dot{\tau}$, of 0.0355 μ/sec. Prior to these

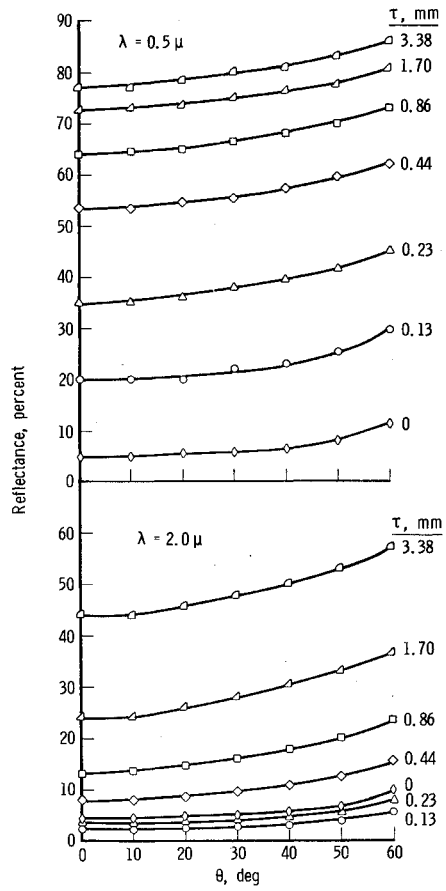

Fig. 4 Reflectance as a function of view angle for CO_2 deposits formed on a black epoxy paint substrate.

¶ Additional experimental data are contained in Ref. 6.

measurements, the test surface was cleaned and recoated with fresh black epoxy paint which had a slightly lower reflectance from that shown in Fig. 2. The reflectances of the thin deposits are shown in Fig. 5 for the wavelength range from 0.5 to 5.0 μ and for thicknesses of 2, 27, 54, 108, and 215 μ. Notice that even for the thinnest deposit, 2 μ, the 4.3 μ anomalous dispersion peak is already quite apparent. The only other significant change in reflectance for all thicknesses and wavelengths is the gradual increase in reflectance for wavelengths between 0.5 and 1.5 μ due to internal scattering. In the thickness region of overlap between Figs. 2 and 5 it appears that the deposits formed at the lower deposition rate are less reflecting. For example the 231 μ deposit formed at the larger deposition rate has a reflectance of about 32% at $\lambda = 0.5$ μ while the 215 μ deposit formed at the lower deposition rate has a reflectance of only 21% at the same wavelength. For the 2 μ thick deposit, the reflectance is lower than the bare substrate reflectance for wavelengths less than 1 μ. This effect is usually present for all wavelengths although it is not so noticeable in Fig. 5. The deposition pressure for the lower deposition rate varied from 10^{-3} torr for the 2 μ thick deposit up to 2×10^{-2} torr for the 215 μ thick deposit and was a little lower than for the deposits formed at the higher deposition rate.

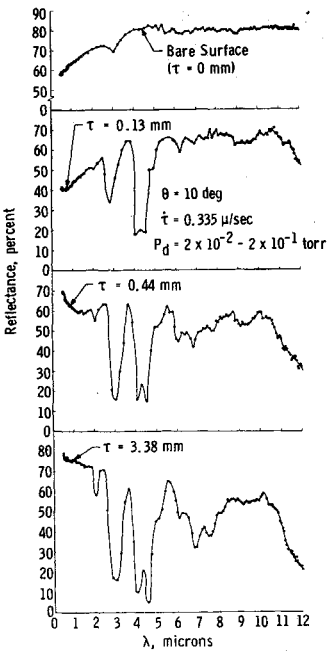

Fig. 6 Reflectance of CO_2 cryodeposits formed on a stainless steel substrate.

Stainless Steel Substrate

The radiative properties of CO_2 deposits were also investigated using a polished LN_2-cooled stainless steel substrate. This was the same test surface employed in the previous measurements but with the black paint removed and the surface repolished. In Fig. 6 the curve labeled $\tau = 0$ mm shows the reflectance of the bare polished stainless steel surface. It is seen that an absorption band occurs around 3.0 μ. This band could not be eliminated although various methods were attempted such as mild bake out under vacuum, repolishing with various types of abrasives, and finally, cleaning with freon in an ultrasonic bath. Since the band shows up at 3.0 μ and increased scatter occurs in the reflectance data for the 5 to 6 μ region, it would appear that some form of water was permanently entrenched in the steel. As seen in Fig. 6, CO_2 deposits of 0.13, 0.44, and 3.38 mm thicknesses were formed on the stainless steel substrate. The pressure during deposition varied from 2 to 4×10^{-2} torr for the 0.13–0.44 mm-thick deposits, and was 2×10^{-1} torr for the 3.38 mm-thick deposit. Notice that for the 0.13 mm deposit the reflectance at the shorter wavelengths ($\lambda = 0.5$ μ) has decreased from the bare substrate reflectance of 58% to 40%. Further increase in deposit thickness, however, causes the reflectance to rise due to internal scattering. For longer wavelengths, $\lambda > 2.0$ μ, the reflectance is influenced by strong absorption bands in some regions, and a gradual decrease in the reflectance is noted in other wavelength regions as the thickness is increased. It was expected in these weakly absorbing regions that the reflectance would gradually decrease with thickness since only a slight increase in reflectance was seen for similar thicknesses of deposits formed on the black surface. In contrast to the reflectance curves for the black epoxy paint substrate, the absorption bands seen in Fig. 6 are quite pronounced even for the smaller deposit thicknesses. In the wavelength regions near these bands the deposits are somewhat transparent with the result that the stainless steel substrate reflectance continues to influence the amount of radiation reflected. The high reflectance at these wavelengths accenuates the absorption bands.

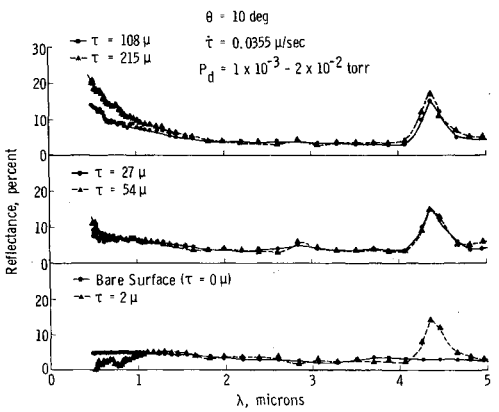

Fig. 5 Reflectance of relatively thin CO_2 cryodeposits formed on a black paint substrate at $\dot{\tau} = 0.0355$ μ/sec.

By comparing the reflectance data for deposits formed on the two substrates, it becomes apparent that the CO_2 deposits transmit appreciably in the wavelength region from 1 to 12 μ. If the deposits were not somewhat transparent, the reflectances observed for cryodeposits of equal thickness formed on the two different substrates would be more nearly the same. For instance, the reflectance at 5.5 μ for a 3.38-mm thick deposit on stainless steel is 65% whereas for an equal thickness on the black substrate the reflectance is only 19%. This indicates that even at this relatively large thickness the substrate reflectance still influences the reflectance of the cryodeposit-substrate complex which can only be explained by the deposit being transparent for radiation at these wavelengths.

As mentioned previously, the absorption bands of CO_2 show up more clearly in Fig. 6 than in Fig. 2. Absorption bands for the 3.38 mm-thick deposit can be seen to be centered around 2.0, 2.85–3.0, 4.3, 6.1, 6.85, and 7.55 μ. The location of the absorption band in the 2.85–3.0 μ region seemed to vary with deposits. For instance in Fig. 6 with $\tau = 0.13$ mm the band is centered at 2.85 μ whereas thicker deposits exhibited the same absorption band centered at 3.0 μ. This variation was also seen for other deposits (not presented). As shown in Fig. 6, the reflectance peak at 4.3 μ is again present but is not so noticeable as in Fig. 2. Notice, however, that the peak heights are about the same in each case (20–25%). For wavelengths between 10 and 12 μ, there is a significant reduction in reflectance. At a deposit thickness of 3.38 mm the reflectance has dropped to 25% at 12.0 μ.

The reflectance dependence on view angle for a 0.84 mm-thick CO_2 deposit on stainless steel is presented in Fig. 7. This dependence is significant for $\lambda = 0.5$ and 1.0 μ. However, for the longer wavelengths, there was relatively little

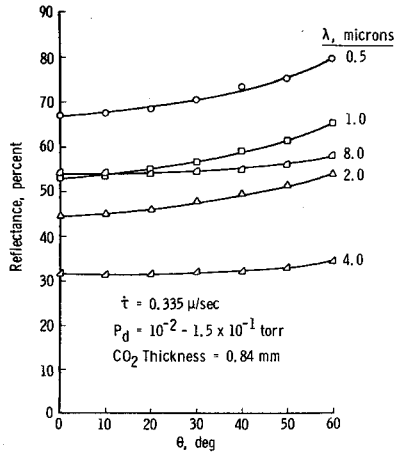

Fig. 7 Reflectance as a function of view angle for CO_2 deposits formed on a stainless steel substrate.

variation with view angle for any of the deposits formed on the stainless steel substrate. This is in contrast with the results obtained using the black substrate which showed a significant dependence on view angle for nearly all wavelengths and deposit thicknesses.

Figure 8 shows how relatively thin CO_2 deposits affect the reflectance of a polished stainless steel surface at wavelengths from 0.5 to 5 μ. As can be seen, the bare stainless steel surface had a reflectance somewhat less than that shown in Fig. 6 due to its optical finish being of lower quality. Deposits of 3.0, 59, and 218 μ thick were formed on this surface at the lower deposition rate, 0.0355 μ/sec. Notice that the reflectance changes significantly even for the thin deposits. For the 3.0 μ thick deposit, thin film interference patterns are seen along with an over-all reflectance reduction of about 5 to 10% from that of the bare surface. For the 59 μ thick deposit, the interference patterns are gone but the reflectance has been decreased further. The absorption bands at 2.85 and 4.3 μ also are seen to be already quite strong for the 59 μ thickness. For the 218 μ thick deposit, the reflectance is reduced even more and the strength of the absorption bands is greater.

The data presented in Figs. 6–8 are for CO_2 deposits formed in layers. Figure 9 shows the variation of reflectance with thickness for a CO_2 deposit formed continuously on the stainless steel substrate. These measurements were made at a wavelength of 0.705 μ for a view angle of 18°. The reflectance of the bare stainless steel substrate was essentially the same as that shown in Fig. 8 for $\lambda = 0.705$ μ. It is seen in Fig. 9 that as the deposit thickens the experimental reflectance has a sharp initial decrease, followed by a more gradual decrease until it reaches a minimum and then it increases until it levels off at a value much higher than the bare surface reflectance. This reflectance behavior with deposit thickness will be explained in detail in the next section where a theoretical study is made.

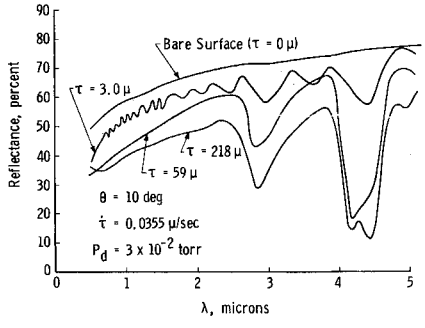

Fig. 8 Reflectance of relatively thin CO_2 cryodeposits formed on a stainless steel substrate at $\dot{\tau} = 0.0355$ μ/sec.

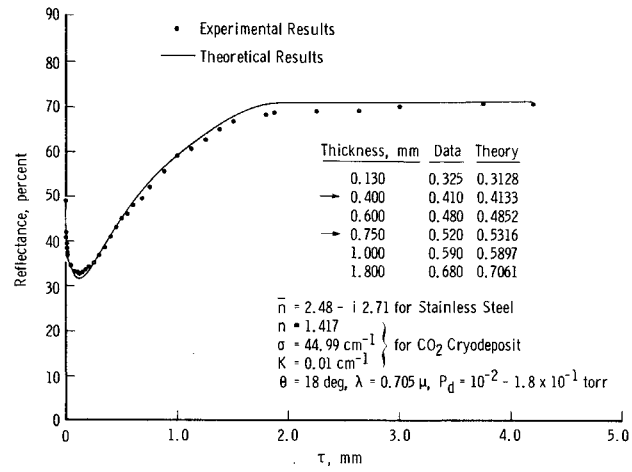

Fig. 9 Comparison of experimental and theoretical reflectance results for CO_2 deposits formed continuously on a stainless steel substrate, $\lambda = 0.705$ μ.

Analytical Results

As mentioned previously, Fig. 9 shows that the experimental reflectance initially undergoes a decrease, then descends to a minimum and finally increases with deposit thickness until reaching a plateau. Because of this interesting behavior an analytical investigation was conducted to obtain a fundamental understanding of cryodeposit reflectances and their variation with thickness. The theoretical study was conducted with the objective of formulating a mathematical model for the cryodeposit reflectance based on the results of the present experimental work. In the search for a realistic reflectance model several combinations of boundary conditions were considered for the substrate and vacuum deposit interface. Based on the magnitude of the reflectances and the general trend of the data presented in this report and in Ref. 1, it was decided that the best model would be to consider the substrate and vacuum deposit interfaces as Fresnel surfaces. The internal structure of the deposit was considered as an absorbing and isotropic scattering medium.

This model for the cryodeposit reflectance required the solution of the radiative transport equation

$$\frac{dI(\bar{\tau},\mu)}{d\bar{\tau}} = -\frac{I(\bar{\tau},\mu)}{\mu} + \frac{W}{2\mu}\int_{-1}^{1} I(\bar{\tau},\mu')d\mu' \qquad (2)$$

where $\bar{\tau}$ is the local optical depth, μ is the cosine of the angle defining the direction of the local intensity $I(\bar{\tau},\mu)$ and W is the albedo parameter, $\sigma/(\sigma + K)$, with σ and K being the scattering and absorption coefficients, respectively. The transport equation, which is for monochromatic radiation, is an integro-differential equation and was reduced to a system of ordinary linear differential equations by the method of discrete ordinates which employed the Gaussian quadrature

$$\int_{-1}^{1} f(x)dx = \sum_{j=1}^{m} f(x_j)a_j \qquad (3)$$

where x_j is the quadrature point and a_j is the quadrature weight. Therefore, Eq. (2) becomes

$$\frac{dI(\bar{\tau},\mu_i)}{d\bar{\tau}} = -\frac{I(\bar{\tau},\mu_i)}{\mu_i} + \frac{W}{2\mu_i}\sum_{j=1}^{m} I(\bar{\tau},\mu_j)a_j \qquad i = 1,2,..,m \qquad (4)$$

The solution of this system of simultaneous differential equations together with the diffuse irradiance boundary conditions is extremely lengthy and complex and is discussed in detail in Ref. 8. It should suffice to mention that the system

of equations was solved numerically using the Milne predictor-corrector method. For a given optical thickness, the computation time required to obtain a solution of Eq. (4) with $m = 10$ and $W = 1.0$ was 30 sec or less on an IBM 360 Model 50 digital computer.

The theoretical investigation was conducted with the point of view of matching the experimental reflectance of cryodeposits as a function of deposit thickness. This led to a computer program that employs two experimental data points (the reflectance at two different thicknesses) to calculate a monochromatic absorption coefficient K and scattering coefficient, σ. In order to arrive at a K and σ, the refractive indices of both the cryodeposit and substrate were required. The refractive index n of the CO_2 deposit at $\lambda = 0.705$ μ was (Ref. 3) 1.417 and the refractive index $\bar{n}$ used for the stainless steel substrate was $2.48 - i2.71$ which corresponds to the reflectance of the bare stainless steel surface in Fig. 9. Once the absorption and scattering coefficients were calculated from the two data points** they were used to "predict" reflectance values at each deposit thickness. Figure 9 shows a comparison between the theoretical and measured reflectance for the CO_2 cryodeposit formed continuously on stainless steel. Both the theoretical and experimental results are for $\lambda = 0.705$ μ and $\theta = 18°$. The arrows on the figure indicate the two data points used in the computer program to calculate the monochromatic absorption and scattering coefficients. All theoretical points were predicted using these coefficients. As seen in Fig. 9, the theoretical results are in good agreement with the data which indicates that the analytical model proposed is realistic. No comparisons were made between theory and data for the results presented in the other figures because the refractive indices of both the deposit and substrate were not known at the other wavelengths and hence the spectral scattering and absorption coefficients could not be inferred.

Since the cryodeposit reflectance model has proven to be a reasonable one, it can be used to explain the thickness dependence of the experimental data in Fig. 9. For small deposit thicknesses near zero, there is a sharp (almost discontinuous) drop in reflectance due to the relative refractive index change.†† This reflectance decrease is from 49% to 39% and is denoted as the first decrease. As the deposit thickness increases there is a second reflectance decrease from 39% to 32.5%. In view of the theoretical model, this second decrease is a result of internal scattering occurring in the deposit. Some of the internally scattered intensity is incident internally on the vacuum-deposit interface at angles greater than the critical angle and undergoes total internal reflection. The reflectance decreases since the thickness increase causes a higher probability that more intensity will be scattered past the critical angle and eventually will be absorbed by the substrate before being rescattered. As the thickness increases further, the total internally reflected intensity has an even higher probability of being rescattered before reaching the substrate and being rescattered into directions less than the critical angle and hence partially escaping the cryodeposit. At larger thicknesses the internal scattering dominates causing more intensity to escape the deposit due to the rescattering effect and resulting in a reflectance that monotonically increases with thickness. For these layers each ray is multiscattered and thus less likely to reach the substrate. For greater deposit thicknesses, the curve levels off at a reflectance plateau of about 71%. The reflectance should stay at approximately this value as the thickness increases further since there is a finite amount of absorption.

** The computation time required to solve for these coefficients by iteration was approximately 10 min.

†† Relative refractive index change also causes the initial reflectance drop observed for the thin CO_2 deposits on the black paint substrate.

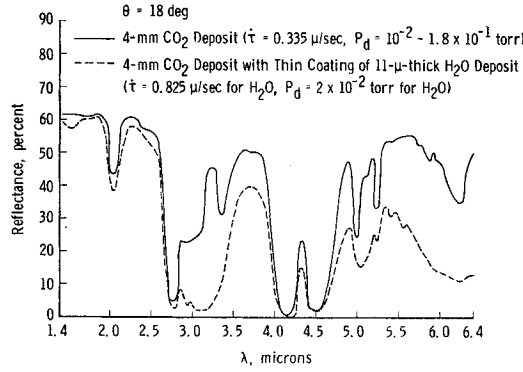

Fig. 10 Reflectance of a 4-mm CO_2 deposit on stainless steel with and without an 11-μ-thick H_2O layer on the CO_2.

Discussion

Possible applications of the results in Figs. 2–9 to some of the problems mentioned in the introduction are apparent. The presence of thin CO_2 deposits ($\tau < 100$ μ) on black surfaces will have a relatively small effect; the reflectance in the visible and near infrared wavelength range will show only a slight increase and for infrared radiation the reflectance will be reduced for these same thicknesses. For even thinner deposits, $\tau < 20$ μ, the reflectance in the visible and near IR can also be reduced. For most applications in space simulation chambers these changes will be negligible. The reflectance changes for the larger thicknesses ($\tau > 100$ μ), however, will not be negligible.

The thin deposits may also have a significant effect in the calibration of low-temperature black body reference sources. The presence of thin deposits will, in general, increase the emittance, especially in the wavelength range from 3.0 μ to 12.0 μ. Although no data were taken for $\lambda > 12.0$ μ it is believed that emittance values would also be increased for longer wavelengths.

Cooled optics are often used in situations where the surrounding pressure is relatively high, e.g., in ballons or aircraft. Under such conditions it is impossible to keep cryogenically cooled surfaces free from contamination due to condensation of CO_2 and H_2O gases. For determination of effects of the CO_2 frosts on cooled optics (such as mirrors), Fig. 8 summarizes some of the problems that would be encountered. For example, the 3.0 μ thick deposit formed on a polished stainless steel surface causes the reflectance to decrease overall and to vary with wavelength because of the phenomenon of thin film interference. These interference peaks and valleys were seen for deposits up to approximately 10 μ thick. This phenomenon would cause a similar wavelength dependent increase and decrease in the transmission of cooled windows and lenses. For a thicker deposit, 59 μ, the reflectance is reduced by about 10–15% over most of the wavelength range from 0.5 to 5.0 μ. In the region of the 2.85 and 4.3 μ absorption bands the reflectance as expected is reduced considerably more. It may be concluded from Fig. 8 that deposits thicker than 60 μ will render a cooled optical surface unusable at wavelengths less than 5 μ.

Finally, the findings of the Mariner 6 and 7 probes and the missions of the upcoming Mars orbiters have increased the interest in the reflective properties of both CO_2 and H_2O frosts. According to Herr and Pimentel[9] the reflection spectra obtained by Mariners 6 and 7 indicate that the Martian polar caps are CO_2. They also reported that absorption bands at 3.34 and 3.04 μ, which had initially been designated by them as methane and ammonia bands, respectively, were also due to CO_2. They verified this by obtaining the same absorption bands for CO_2 frosts formed under laboratory conditions. This was the first reported observation of these two bands for CO_2. These two bands were not seen in the measurements

presented in Figs. 2 and 6 and the data in Fig. 6 were, like the laboratory data of Herr and Pimentel, for CO_2 formed on stainless steel.

In order to obtain higher resolution data than shown in Fig. 6, the NaCl prism in the monochromator was replaced by a CaF_2 prism. Figure 10 shows the reflectance results for a CO_2 deposit 4 mm thick. The pressure during deposition was 1.80×10^{-1} torr or less and the view angle, θ, was 18°. With the higher resolution an absorption band was seen at approximately 3.36 μ which is probably the same band reported by Herr and Pimentel.[9] The other band reported by Herr and Pimentel at approximately 3.04 μ was not seen. The anomalous dispersion reflectance peak at 4.3 μ was not observed in the reflection spectra of the Martian polar cap shown by Herr and Pimentel.[9] However, in a later article[10] they report seeing the anomalous dispersion peak at 4.3 μ but not while viewing the polar caps but when viewing the bright limb of the planet. Based on our results we feel their observation of the 4.3 μ peak establishes conclusively the presence of solid CO_2 either on the surface or in the atmosphere of Mars.

As seen in Fig. 10 for the 4 mm CO_2 deposit, there is a broad absorption band centered around 3.0 μ which is probably due to a small trace of water that was present in the chamber from outgassing. The band centered around 6.2 μ also indicates the presence of water impurities even though the chamber was initially pumped down to approximately 5×10^{-7} torr. To determine the effect of water contamination, a thin film of water frost ($\tau = 11$ μ) was formed on top of the 4 mm thick CO_2 deposit. Figure 10 shows the results. Even for this small thickness, the reflectance was reduced for all wavelengths with the most noticeable reductions occurring in the 2.9 to 3.4 μ region and the 4.8 to 6.4 μ range. This means that the 3.04 μ band seen in Ref. 9 would not appear in Fig. 10 due to the trace of water which obscured any recognizable band in this wavelength region. It is also seen in Fig. 10 that the band at 3.36 μ is eliminated after formation of the thin water film. This may be the reason that the band had not been observed previously since only a small amount of water contamination could mask its appearance.

Summary

In situ reflectance measurements on LN_2-cooled surfaces within a vacuum were carried out in a powdered sodium chloride coated integrating sphere. The wavelength range investigated was from 0.5 to 12.0 μ. Reflectance measurements of CO_2 cryodeposits formed on black epoxy paint coated and stainless steel surfaces were obtained for deposit thicknesses ranging from 2 μ to 4.0 mm. A reflectance peak at 4.3 μ was found to be due to anomalous dispersion. The presence of this peak in reflection spectra was shown to be a very sensitive method of detecting solid CO_2 since a deposit only 2μ thick on black epoxy paint shows the peak quite clearly.

CO_2 deposits were seen to absorb strongly at 2.0, 2.85, and in the vicinity of 4.3 μ. With a higher resolution instrument, weaker absorption bands were also seen at 3.36, 5.0 and 5.24 μ. Thick CO_2 deposits were highly reflecting at the shorter wavelengths ($\lambda < 2.0$ μ) and transmit appreciably at longer wavelengths (excluding absorption bands). The reflectance was found to be dependent on view angle for all wavelengths for CO_2 formed on the black epoxy paint. Less dependence on view angle was seen for the deposits formed on the stainless steel substrate. The experimental reflectance was also found to have a strong dependence on deposit thickness and substrate. In one instance, an analytical model was used to predict the reflectance as a function of CO_2 deposit thickness on stainless steel. The agreement between the theoretical and experimental results was quite good.

Finally, the applicability of the experimental results to several current problems was discussed. These included: determination of the composition of the Martian polar caps, thermal radiative properties of cooled optics, effects on space simulation chamber cold walls, and effects on emittance of low-temperature black body reference sources.

References

[1] McCullough, B. A., Wood, B. E., Smith, A. M., and Birkebak, R. C., "A Vacuum Integrating Sphere for In Situ Reflectance Measurements at 77°K from 0.5 to 10 μ," *AIAA Progress in Astronautics and Aeronautics: Thermophysics of Spacecraft and Planetary Bodies*, Vol. 20, edited by Gerhard B. Heller, Academic Press, New York, 1967, pp. 137–150.

[2] Kneissl, G. J., Richmond, J. C., and Wiebelt, J. A., "A Laser Source Integrating Sphere for the Measurement of Directional Hemispherical Reflectance at High Temperatures," *AIAA Progress in Astronautics and Aeronautics: Thermophysics of Spacecraft and Planetary Bodies*, Vol. 20, edited by Gerhard B. Heller, Academic Press, New York, 1967, pp. 177–202.

[3] Seiber, B. A., Müller, P. R., Smith, A. M., and Wood, B. E., "Refractive Indices and Densities of CO_2 and H_2O Cryodeposits," ASME Paper 70-HT-33, Detroit, Mich., 1970.

[4] Smith, A. M., Tempelmeyer, K. E., Müller, P. R., and Wood, B. E., "Angular Distribution of Visible and Near IR Radiation Reflected from CO_2 Cryodeposits," *AIAA Journal*, Vol. 7, No. 12, Dec. 1969, pp. 2274–2280.

[5] Wood, B. E. and Smith, A. M., "Spectral Reflectance of Water and Carbon Dioxide Cryodeposits from 0.36 to 1.15 μ," *AIAA Journal*, Vol. 6, No. 7, July 1968, pp. 1362–1367.

[6] Wood, B. E., Smith, A. M., Seiber, B. A., and Roux, J. A., "Infrared Reflectance of CO_2 Cryodeposits," TR-70-108 (AD-708509), July 1970, Arnold Engineering Development Center, Arnold Air Force Station, Tenn.

[7] Jenkins, F. A. and White, H. E., *Fundamentals of Optics*, McGraw-Hill, New York, 1957, pp. 469–477.

[8] Roux, J. A., "Radiative Heat Transfer of Coatings on a Cryogenic Surface," Ph.D. dissertation, 1970, Univ. of Tennessee.

[9] Herr, K. C. and Pimentel, G. C., "Infrared Absorptions Near Three Microns Recorded Over the Polar Caps of Mars," *Science*, Vol. 166, No. 3904, Oct. 24, 1969, pp. 496–499.

[10] Herr, K. C. and Pimentel, G. C., "Evidence for Solid Carbon Dioxide in the Upper Atmosphere of Mars," *Science*, Vol. 167, No. 3914, Jan. 2, 1970, pp. 47–49.